

Transition from non-resonant to resonant random lasers by the geometrical confinement of disorder

N. Ghofraniha^{1,*}, I. Viola², A. Zacheo³, V. Arima⁴, G. Gigli⁵ and C. Conti⁶

¹ *Institute for Physical Chemical Processes (IPCF-CNR), UOS Roma Kerberos, Università La Sapienza, P. le A. Moro 2, I-00185, Rome, Italy*

² *National Nanotechnology Laboratory, Institute Nanoscience-CNR (NNL, CNR-NANO), I-73100 Lecce, Italy and c/o Department of Physics, La Sapienza University, Rome, Italy*

³ *Dip. di Matematica e Fisica "Ennio de Giorgi", Università del Salento, I-73100, Lecce, Italy*

⁴ *National Nanotechnology Laboratory, Institute Nanoscience-CNR (NNL, CNR-NANO), I-73100 Lecce, Italy*

⁵ *National Nanotechnology Laboratory, Institute Nanoscience-CNR (NNL, CNR-NANO), Lecce, Italy and c/o Department of Physics, La Sapienza University, Rome; Università del Salento, Dip. di Matematica e Fisica "Ennio de Giorgi" and Italian Institute of Technology (IIT), Centre for Biomolecular Nanotechnologies, Lecce, Italy*

⁶ *Institute for Complex Systems (ISC-CNR) and Department of Physics, University Sapienza, P.le A. Moro 5, I-00185, Rome, Italy*

* *neda.ghofraniha@roma1.infn.it*

Compiled July 8, 2021

We report on a novel kind of transition in random lasers induced by the geometrical confinement of the emitting material. Different dye doped paper devices with controlled geometry are fabricated by soft-lithography and show two distinguished behaviors in the stimulated emission: in the absence of boundary constraints the energy threshold decreases for larger laser volumes showing the typical trend of diffusive *non-resonant* random lasers, while when the same material in lithographed into channels, the walls act as cavity and the *resonant* behavior typical of standard lasers is observed. The experimental results are consistent with the general theories of random and standard lasers and a clear phase diagram of the transition is reported. © 2021 Optical Society of America

OCIS codes: 000.0000, 999.9999.

Inhomogeneity of refractive index in materials provokes the scattering of electromagnetic waves with wavelength λ comparable to the characteristic size of the refraction variation. While ordered distribution of the scatterers gives rise to the typical wave interference fringes known as Bragg diffraction, disordered distribution induces the random propagation of light in space and a more complex interference pattern. This simple effect has promoted in the last decades the development of random photonics with novel fascinating physical phenomena and relevant applications [1]. Among all, the severe effects of disorder have been widely investigated in nonlinear optical wave propagation, as shock waves [2, 3], beam filamentation [4] and soliton formation [5]; moreover ultra-focusing of light through disordered media is nowadays paving the way to novel imaging techniques [6] and Anderson localization of light in the regime of high scattering strength has been considered [7–9]. Another intriguing effect of “disordered light” is represented by random lasers (RLs), that are light sources made by a gain medium whose spontaneous emission is amplified by the feedback mechanism due to multiple scattering. This is achieved by adding powders or nano-particles [10, 11] or by the intrinsic supramolecular structure of the gain material [12]. Depending on the emission properties two main groups of RLs have been classified: RLs with intensity non-resonant feedback characterized, above the threshold, by a drastic narrowing of the emission spectrum in a broad and featureless peak centered at the

highest gain frequency; RLs with field resonant feedback, presenting multiple sub-nanometer narrow peaks above the amplification line. Mainly, the formers have been realized in weakly scattering materials with $l_t \gg \lambda$, with l_t the transport mean free path, and the latter in highly scattering systems with $l_t \geq \lambda$. Interesting exceptions have also been reported signaling the crucial role of the pump size, shape [13] and direction [14] as well as the amplifying material [15]. Hence, the classification of RLs is still an open question. More generally, when $l_t \lesssim \lambda/2\pi$, the separated emission peaks are monochromatic and identified with the localized and long-lived eigenmodes of the Maxwell’s equations in the passive system [16–18]. However, this situation is experimentally hardly obtainable especially in 3-dimensional materials and most of the experiments reporting resonant peaks are far from this regime. In all other scattering regimes the eigenmodes are not standing waves with defined phase but are short-lived “quasimodes”, a subset of which can give life to spatially extended lasing modes across the pumped system [19]. The scattering strength and/or pumping conditions control the spatial extension of such subset: in the case of a large number of equally excited activated modes, they merge to a continuous broadband; while in the situation of a reduced amount of modes, the emission spectra present few distinguishable non-monochromatic resonances.

In this Letter we introduce a novel kind of resonance in weakly scattering RLs, that is not due to the partial

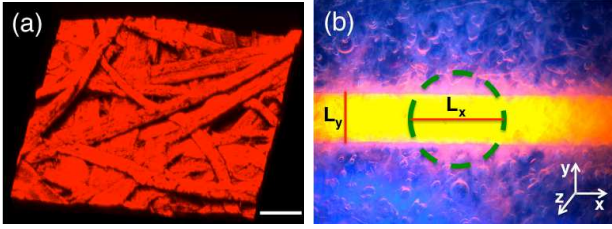


Fig. 1. (Color online) (a) Confocal microscopy image (3-D reconstruction) showing the paper mash impregnated by dye solution, the scale bar is $50\mu\text{m}$. (b) Fluorescence image of the micro-fluidic channel with $L_y=300\mu\text{m}$, the dashed circle indicates the pump spot with diameter L_x .

localization of the extended lasing modes, leading to a fine spectral structure, but is induced by the geometrical confinement of the RL material in micro-channels. Our system is an innovative type of RL made of paper channels impregnated by a dye solution, the micro-fluidic channels are realized by soft lithographic methods, that allow the fine control of their size. Although we observe single broad laser peaks in all cases, being the sample weakly scattering with $l_t = (36 \pm 4)\mu\text{m}$, we show that there is a net transition in the behavior of the lasing threshold once the RL is geometrically confined and we report a clear phase diagram of the laser threshold versus sample volume. When the paper is without channels the typical RL behavior [20] is observed while in presence of the channels the threshold energy trend shows the characteristics of a standard laser with the channel walls acting as resonator. By recalling the same definitions introduced by Letokhov in 1968 in the first presentation of “quantum generators” [21], we name this transition: *non-resonant* (random laser) to *resonant* (standard laser).

Our samples are made of chromatographic paper impregnated by a 1mM solution of Rhodamine B and Ethylene-glycol and they all have a thickness of $L_z = 100\mu\text{m}$. Once in contact, for capillarity, the fluid dye solution diffuses inside the mash of the paper filling all the volume available, giving rise to a homogeneous material able to emit radiation because of the dye presence and to scatter the light because the paper is made of cellulose with a typical index refraction of 1.47 at the visible frequencies. We estimate a light mean transport path of $l_t = (36 \pm 4)\mu\text{m}$ at 532 nm wavelength by measuring the transmittance of the paper for various L_z and fitting it with exponential decay. A representative confocal microscopy image of the microscopic structure is shown in fig. 1-a.

Soft lithographic techniques [22, 23] are used to fabricate different microfluidic channels with controlled width L_y of 200 μm , 300 μm and 600 μm , an example is illustrated in fig. 1-b and details of the fabrication are given elsewhere. We use confocal microscopy both to check the homogeneous distribution of the dye solution, by measuring the fluorescence spectra at several points of the samples along the x , y , z directions, and to estimate

the effective thickness of the dyed paper $L'_z < L_z$ due to the capillarity effect. This is obtained by measuring the depth of fluorescence from the z -stack confocal images with a precision of 3 μm .

The samples are pumped along the z direction by a frequency doubled Q-switched Nd:YAG pulsed laser emitting at $\lambda=532\text{ nm}$, with 10 Hz repetition rate, 6 ns pulse duration and with 8 mm beam diameter. In all the measurements the laser is focused down to a spot of diameter $L_x = 600\mu\text{m}$ (see fig. 1-b) and the transmitted radiation is collected after pump filtration and focalization into an optic fiber connected to a spectrograph equipped with electrically cooled CCD array detector. To avoid bleaching effects, we mount our samples on a translator with micro metric control and take each single pulse emission spectrum from a distinct point of the channels. No pulse to pulse variations in the emission are observed for fixed pumping.

We estimated the absorption and emission cross sections of the dye solution respectively as $\sigma_a = \alpha/N \simeq 1.7 \cdot 10^{-16}\text{cm}^2$ and $\sigma_e = g/N \simeq 5 \cdot 10^{-17}\text{cm}^2$, being the measured absorption $\alpha = 10\text{mm}^{-1}$, the gain coefficient $g \simeq 30\text{ cm}^{-1}$ (assuming that a 1% in volume of Rhodamine B solution in diethylene-glycol at 0.5 nJ/ μm^2 has a gain of 100 cm^{-1} , as measured in [24]) and the dye molecule number density $N \simeq 6 \cdot 10^{17}\text{ cm}^{-3}$. Moreover the paper samples are isotropic as evidenced by the investigation of the scattered intensity at different angles.

We report in fig. 2-a the emission spectra from the sample with $L_y = 300\mu\text{m}$ for various injected energy densities (i.e. energy devided to the pump area). The RL coherent emission is clearly shown by the growth of the peak height by two orders of magnitude and by its narrowing for increasing pump, as illustrated in fig. 2-b.

The single wide emission peak signals the extension of many lasing modes over the pumped volume, as expected for typical weakly scattering RLs. From the trend of the peak intensity it is clear that there is a threshold in the pump energy between the slow growth of the spontaneous emission at low energy and the fast linear increase of the stimulated radiation. In fig. 3-a we illustrate the peak intensity versus input energy density for the different fabricated samples with different geometry: the three lithographed channels described above and two non-lithographed bulk paper pieces with different widths L_y as shown on the figure. The dependence of the laser threshold is strongly affected by the geometry. From the intersection of the two linear curves, fitting the data, we estimate the threshold energy density E_{th} and in fig. 3-b we show it versus the volumes of the different RLs. We first consider the case without channels. We calculate the volumes of the pumped region for the two bulk paper pieces as cylindric volume $V = \pi(L_x/2)^2 \times L'_z$. The data for each sample are given in table 1

To explain the differences of the volumes, we remark that for the bulk papers we use different widths to change the effective depth L'_z and thus the lasing volume: by increasing the width, the dyed fluid penetrates more deeply

Table 1. Sample parameters

Type	L_x (μm)	L_y	L'_z (μm)	V ($10^6 \mu\text{m}^3$)	E_{th} (mJ/m^2)
Bulk	600 ± 5	$(20.0 \pm 0.5) \text{mm}$	85 ± 3	24 ± 1	0.5 ± 0.2
Bulk	600 ± 5	$(3.0 \pm 0.5) \text{mm}$	75 ± 3	21 ± 1	0.6 ± 0.1
Channel	600 ± 5	$(600 \pm 3) \mu\text{m}$	65 ± 3	18 ± 1	0.9 ± 0.1
Channel	600 ± 5	$(300 \pm 3) \mu\text{m}$	60 ± 3	10.8 ± 0.7	0.45 ± 0.07
Channel	600 ± 5	$(200 \pm 3) \mu\text{m}$	45 ± 3	5.4 ± 0.5	0.01 ± 0.03

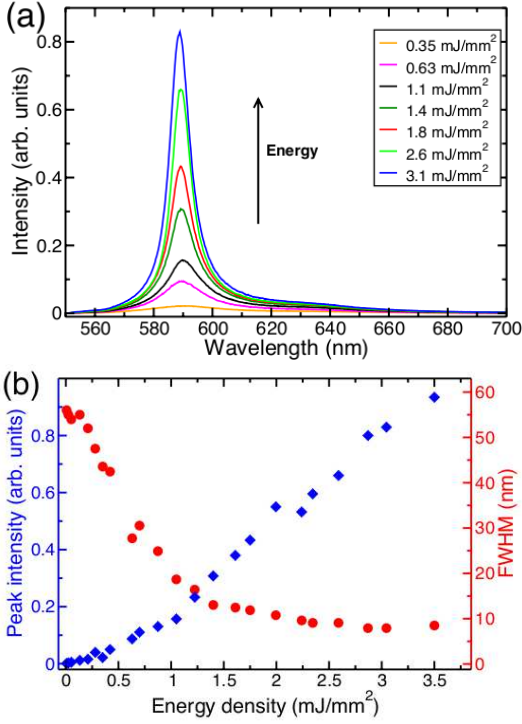


Fig. 2. (Color online) Emission spectra at different pump energy density for the $300 \mu\text{m}$ thick sample (a) and corresponding peak intensity (blue diamonds) and line width (red circles) vs. pump energy (b).

along z inside the paper due the capillarity effect. For the lithographed channels, we calculate the volume of cylinder with $V = \pi(L_x/2)^2 \times L'_z$ for $L_y = 600 \mu\text{m}$ and of parallelepiped with $V \simeq L_x \times L_y \times L'_z$ for $L_y = 200 \mu\text{m}$ and $L_y = 300 \mu\text{m}$.

In fig. 3-b two district regimes are evident: without channels E_{th} decreases by increasing V as expected for typical RLs, where by increasing the gain volume light travels a longer path due to more scattering events and the process of photon generation is amplified. Thus, by enlarging the laser volume the losses are more compensated and the threshold is lowered [20]. This effect has been quantified by Lethokov [21, 25] by considering the diffusive motion of photons in a scattering medium and consequently by solving the diffusion equation for photon

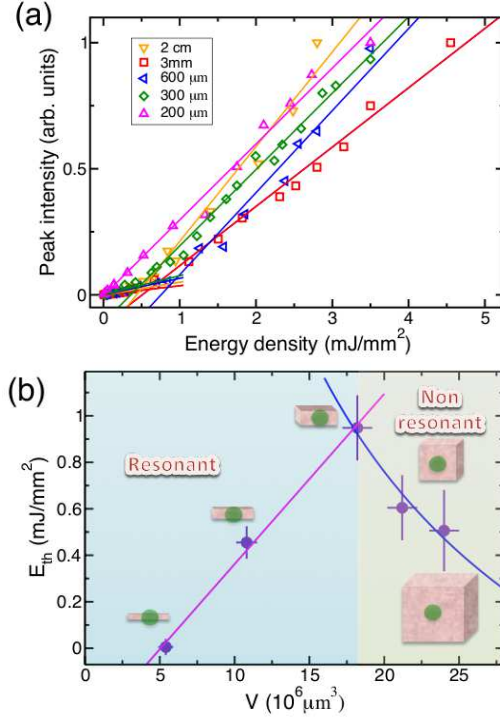


Fig. 3. (Color online) (a) Peaks of the emitted intensity spectra vs. pump energy density for samples with different thickness showing different laser thresholds; solid lines are the linear fitting curves. (b) Energy density threshold E_{th} vs. laser volume V phase diagram showing the resonant - non resonant transition. Sketches of the illuminated volumes are reported: the green spot indicates the pumped volume. Solid lines are the fitting curves after eqs. (4) and (5).

energy density $W(r, t)$ in presence of a uniform gain

$$\frac{\partial W(r, t)}{\partial t} = D \nabla^2 W(r, t) + \frac{v}{l_g} W(r, t) \quad (1)$$

where $D = vl_t/3$ is the diffusion coefficient, v is the photon transport velocity inside the scattering sample and l_g is the gain length (inverse of the gain coefficient g). Equation (1) has the following general solution:

$$W(r, t) = \sum_n a_n \Psi_n(r) e^{-(DB_n^2 - v/l_g)t} \quad (2)$$

that passes from an exponential decay to an exponential

growth at the threshold condition

$$l_g^{th} = \frac{v}{DB_1^2} = \frac{3}{l_t B_1^2} \quad (3)$$

with B_1 the lowest of the eigenvalues B_n , proportional to the inverse of the average size of the medium $V^{1/3}$. The proportionality between the gain coefficient at threshold $g_{th} = 1/l_g^{th}$ and the threshold energy E_{th} and equation (3) give the following relation

$$E_{th} \propto V^{-2/3}. \quad (4)$$

In fig. 3-b the solid line in the right part is the fitting curve to the data, consistent with the experimental results.

Contrarily if the paper is lithographed in channels an opposite behavior is manifested, that is typical of standard lasers with external feedback (mirrors), where, even though the threshold inversion density results $\Delta N_{th} = 2g_{th}/\sigma$, with σ the transition cross section and $g_{th} = 2\delta_c/L_y$, with δ_c including the contribution of the cavity losses and output coupling, the upper-laser-level population created by the pumping rate is $N_2^{th} \propto P_{th}/V$, proportional to the pump power P_{th} per unit volume, see [26], eq. 10, page 460. This means that for the same pump power, a smaller volume leads to a larger atomic population inversion resulting to the linear relation

$$E_{th} \propto V \quad (5)$$

In fig. 3-b the solid line in the left part is the linear fitting curve to the experimental points, showing the consistency of the general form (5) with our data. Notice that we use equations (4) and (5) as general descriptions of the two distinct trends we observe in the experimental results and these observed trends can be used for the validation of theoretical models.

In summary in fig. 3-b we present a new kind of transition in RLs: from RL where the feedback mechanism is solely given by the scattering effect when it is not geometrically confined and in this sense called *non-resonant*, to RL where the same material, constrained in micro-channels with defined walls acting as cavity, shows a laser-like behavior because a secondary geometric feedback effect dominates, and for this reason named *resonant* RL. In presence of boundaries on the transverse direction, the scattering is strong since the waves cannot escape from the side of the sample and therefore it is easy to achieve wave localization. In other words, the paper channels enhance the scattering effect and the light has a greater probability of returning to the coherence volume and interferes with itself and this gives the resonant behavior. We stress that the channel walls are present only on the y -direction, while in the z -direction the RL (paper+dyer) is between air and pure paper. By investigating the dependence of the pump energy at laser threshold on the laser volume we depict the phase diagram of such transition where the two opposite behaviors of the stimulated emission are clearly shown and

quantified by means of general theories of standard and random lasers. Our results not only evidence the crucial role of geometrical confinement in the physics of disordered lasers, but they also show the potentiality of soft lithographic techniques in realizing cheap paper-based photonic devices and open the way to lab on chip and optofluidic integrated systems [27].

The research leading to these results has received funding from the Italian Ministry of Education, University and Research under the Basic Research Investigation Fund (FIRB/2008) program/CINECA grant code RBFR08M3P4.

References

1. D. S. Wiersma, Nat. Photon. **7**, 188 (2013).
2. N. Ghofraniha, S. Gentilini, V. Folli, E. DelRe, and C. Conti, Phys. Rev. Lett. **109**, 243902 (2012).
3. S. Gentilini, N. Ghofraniha, E. DelRe, and C. Conti, Opt. Express **20**, 27369 (2012).
4. C. Conti, N. Ghofraniha, G. Ruocco, and S. Trillo, Phys. Rev. Lett. **97**, 123903 (2006).
5. V. Folli and C. Conti, Phys. Rev. Lett. **104**, 193901 (2010).
6. I. M. Vellekoop, A. Lagendijk, and A. P. Mosk, Nat. Photon. **4**, 320 (2010).
7. D. S. Wiersma, P. Bartolini, A. Lagendijk, and R. Righini, Nature **390**, 671 (1997).
8. M. Segev, Y. Silberberg, and D. N. Christodoulides, Nat. Photon. **7**, 197 (2013).
9. S. T., W. Buhner, C. M. Aegerter, and G. Maret, Nat. Photon. **7**, 148 (2013).
10. D. S. Wiersma, Nature Phys. **4**, 359 (2008).
11. K. L. van der Molen, R. W. Tjerkstra, A. P. Mosk, and A. Lagendijk, Phys. Rev. Lett. **98**, 143901 (2007).
12. N. Ghofraniha, I. Viola, F. Di Maria, G. Barbarella, G. Gigli, and C. Conti, Laser & Photonics Reviews **7**, 432 (2013).
13. X. Wu and H. Cao, Phys. Rev. A **77**, 013832 (2008).
14. M. Leonetti, C. Conti, and C. Lopez, Nat. Photon. **5**, 615 (2011).
15. S. Mujumdar, M. Ricci, R. Torre, and D. S. Wiersma, Phys. Rev. Lett. **93**, 053903 (2004).
16. C. Vanneste and P. Sebbah, Phys. Rev. Lett. **87**, 183903 (2001).
17. P. Sebbah and C. Vanneste, Phys. Rev. B **66**, 144202 (2002).
18. C. Conti, M. Leonetti, A. Fratalocchi, L. Angelani, and G. Ruocco, Phys. Rev. Lett. **101**, 143901 (2008).
19. C. Vanneste, P. Sebbah, and H. Cao, Phys. Rev. Lett. **98**, 143902 (2007).
20. G. van Soest, M. Tomita, and A. Lagendijk, Opt. Lett. **24**, 306 (1999).
21. V. S. Letokhov, Sov. Phys. JETP **26**, 835 (1968).
22. A. C. Siegel, S. T. Phillips, M. D. Dickey, N. Lu, Z. Suo, and G. M. Whitesides, Adv. Funct. Mater. **20**, 28 (2010).
23. A. W. Martinez, S. T. Phillips, and G. M. Whitesides, Proc. Natl. Acad. Sci. **105**, 19606 (2008).
24. M. Leonetti and C. Lopez, Appl. Phys. Lett. **101**, 251120 (2012).
25. H. Cao, Waves Random media **13**, R1 (2003).

26. A. E. Siegman, *Lasers* (University Science Books, 1987).
27. B. N. S. Bhaktha, N. Bachelard, X. Noblin, and S. P, Appl. Phys. Lett. **101**, 151101 (2012).